Chiara Fania[1]*
Michele Vasso[1,2]*
Enrica Torretta[1]
Paul Robach[3]
Gaetano Cairo[4]
Carsten Lundby[5]
Cecilia Gelfi[1,2]

[1]Dipartimento di Scienze e Tecnologie Biomediche, Università degli Studi di Milano, Milan, Italy
[2]Istituto di Bioimmagini e Fisiologia Molecolare, C.N.R., Segrate, Milan, Italy
[3]Département Médical, Ecole Nationale de Ski et d'Alpinisme, Chamonix, France
[4]Dipartimento di Morfologia Umana e Scienze Biomediche, Università degli Studi di Milano, Milan, Italy
[5]Copenhagen Muscle Research Centre, University of Copenhagen, Copenhagen, Denmark

Received November 15, 2010
Revised April 7, 2011
Accepted April 7, 2011

Research Article

Setup for human sera MALDI profiling: The case of rhEPO treatment

The implementation of high-throughput technologies based on qualitative and quantitative methodologies for the characterization of complex protein mixtures is increasingly required in clinical laboratories. MALDI profiling is a robust and sensitive technology although the serum high dynamic range imposes a major limitation hampering the identification of less abundant species decreasing the quality of MALDI profiling. A setup to improve these parameters has been performed for recombinant human erythropoietin (rhEPO) monitoring in serum, analyzing the effects of two commercially available columns (MARS Hu7 and Hu14) for immunodepletion, and two matrices (α-cyano-4-hydroxycinnamic acid and 2′,4′-dihydroxyacetophenone) for peak quality improvement. The immunodepletion capability of both columns was determined by 2-D DIGE, which precisely revealed the efficacy of Hu14 in protein removal and the serum dynamic range decrement. In addition, the type of matrix, the sample dilution, and the efficacy of optimized parameters were used for serum profiling of ten healthy subjects before and after rhEPO treatment. The principal component analysis indicates that a combination of Hu14 column and 2′,4′-dihydroxyacetophenone matrix increases data quality allowing the discrimination between treated and untreated samples, making serum MALDI profiling suitable for clinical monitoring of rhEPO.

Keywords:
EPO / Immunodepletion / MALDI profiling / Serum / 2-D differential gel electrophoresis
DOI 10.1002/elps.201100134

1 Introduction

More and more proteomic approaches are imposing themselves in clinical studies for qualitative and quantitative investigation related to protein and peptide expression profiles from body fluids and tissue extracts [1]. Moreover, to make these methodologies suitable for clinical practice, it is necessary to isolate and quantify proteins from biological fluids. Currently, proteomic analysis of biological fluids is one of the most promising approaches in biomarker discovery [2]. In particular, serum, the most relevant source of biomarkers [3, 4], is increasingly utilized in clinical proteomic studies [4, 5].

Serum profiling by using surfaced-enhanced laser desorption ionization (SELDI) was utilized to investigate pathological status, particularly breast cancer, for the analysis of low-molecular-weight proteins [6–8]. Surfaced-enhanced laser desorption ionization opened a new avenue in the application of laser desorbed based fingerprinting for clinical diagnosis providing spectra, as fingerprints. The possibility of identifying peaks adopting advanced instrumentation makes MALDI profiling more robust and sensitive [9] due to its high throughput and reliability in protein detection [10]. Both, protein profiles and the single identified protein, can provide disease-specific protein patterns or biomarkers after clinical validation. Despite the strong potential of MALDI, the main issue to face remains the serum dynamic range (i.e. the range of serum protein concentrations from high- to low-abundance proteins, estimated in ten orders of magnitude [11]) which encompasses eight orders of magnitude the capacity of the mass

Correspondence: Professor Cecilia Gelfi, Dipartimento di Scienze e Tecnologie Biomediche, Università degli Studi di Milano, Milan, Italy; Via Fratelli Cervi 93, 20090 Segrate, Milan, Italy
E-mail: cecilia.gelfi@unimi.it
Fax: +39-0221717558

Abbreviations: CHCA, α-cyano-4-hydroxycinnamic acid; **DHAP,** 2′,4′-dihydroxyacetophenone; **DIGE,** differential gel electrophoresis; **HAP,** high-abundant proteins; **Hu7,** Human 7; **Hu14,** Human 14; **LAP,** low-abundant proteins; **MARS,** multiple affinity removal system; **NL,** nonlinear; **PCA,** principal component analysis; **rhEPO,** recombinant human erythropoietin

*These authors have contributed equally to this study.

Colour Online: See the article online to view Figs. 6 and 7 in colour.

spectrometer to discriminate species in complex mixtures [12–15] preventing the detection of biomarkers from picogram to femtogram levels, such as prostate specific antigen (PSA) or interleukins, leaving undisclosed a large number of proteins and peptides. So far, to overcome this issue, an adequate fractionation step prior proteomic analysis is mandatory in order to remove high-abundant components. Several prefractionation methodologies have been introduced such as ultracentrifugation [4, 16], solid-phase extraction (SPE) columns [17–21], size fractionation [22], derivatized beads [23, 24], combinatorial peptide ligand libraries [25], and specific enrichment techniques [26–29]. Moreover, the high cost, the scarce selectivity, or long operation times, impose the development of new depletion systems based on multiple affinity columns [30, 31]. The latter are characterized by the presence of specific antibodies derivatized columns which specifically and selectively deplete a number of high-abundant proteins in serum plus their proteolytic products and molecular forms [32–37]. The selection of a methodological approach providing optimal reduction of the serum dynamic range with high reproducibility represents a critical point for the translation of MALDI serum profiling to clinical laboratories. This study puts forward the development of a robust platform to analyze the effects of recombinant human erythropoietin (rhEPO) treatment in human sera by MALDI.

Erythropoietin is a glycoprotein hormone, mainly secreted by the kidney that, by stimulating red blood cell production, increases oxygenation levels in tissues [38]. The recombinant form of EPO (rhEPO) is largely utilized in patients affected by severe anemia and in the treatment of pathologies associated with low oxygen levels in blood [39, 40]. Furthermore, because of its capability to increase physical performance, this hormone is one of the most used doping agents. The use of rhEPO easily increases red blood cell mass compared with homologous/autologous blood transfusion. For this reason, rhEPO is on the list of prohibited substances of International Olympic Committee (IOC) and World Anti-Doping Agency (WADA) [41]. In a previous study on male volunteers [42], rhEPO administration effectively increased erythropoiesis, hematocrit, hemoglobin, and iron mobilization; therefore, a number of changes in serum profile are expected. Due to the short half-life, detection of rhEPO is associated to its assumption modality and available tests can reveal only chronic and/or massive assumption [43]; hence, the development of tests for monitoring rhEPO and proteins or peptides associated to its intake remains of great interest both for clinical purposes and for antidoping in sport practice.

In this context, the aim of the present study is to investigate the effects of different levels of immunodepletion on dynamic range, to select the type of matrix and deposition and to standardize the methodology for implementing MALDI profiling for the analysis of human serum after treatment of healthy human subjects with rhEPO.

2 Materials and methods

2.1 Chemicals

ACN, trifluoroacetic acid, water, citric acid, L-lysine, iodoacetamide, glycerol, PMSF, and ammonium bicarbonate (AMBIC) were from Sigma-Aldrich (Milan, Italy) and are of the highest purity available; buffers A and B for immunodepletion were from Agilent Technologies (Palo Alto, CA, USA). CHAPS, tris[hydroxymethyl] aminoethane (Tris), SDS, bromophenol blue (BBF), agarose, urea, thiourea, dithiothreitol (DTT), TEMED, methylenebisacrylamide, acrylamide, low-molecular-weight marker, Deep Purple, CyDyes, nonlinear IPG strips, pH gradient 3-10 (18 cm long), and IPG buffer, pH 3–10, were from GE Healthcare (Uppsala, Sweden). α-Cyano-4-hydroxycinnamic acid (CHCA), 2′,4′-dihydroxyacetophenone (DHAP), and peptide calibration standard mixture were from Bruker Daltonics (Bremen, Germany); trypsin was purchased from Promega (Madison, WI, USA) and SYPRO Ruby from Molecular Probes (Eugene, OR, USA).

2.2 Sample collection

2.2.1 Immunodepletion and MALDI profiling setup

Blood samples were obtained from three healthy volunteer male subjects and divided in two aliquots, for serum and plasma collection, respectively. The first aliquot was collected in vacutainer tubes placed at +4°C for 15 min until clotted, then centrifuged for 10 min at $2200 \times g$ at +4°C and stored at −80°C. The second was collected in heparin vacutainer tubes, centrifuged (15 min, $2000 \times g$, +4°C), and stored at −80°C until use.

2.2.2 rhEPO treatment

Sera were obtained from ten healthy young male volunteers. The treatment protocol consisted of epoetin β (NeoRecormon, Roche, Mannheim, Germany) subcutaneous injection once every other day for 2 wks, and then once a week in the third and fourth weeks. The measurements consisted of blood samples taken from a forearm vein during supine rest at baseline (control samples) and on days 2, 4, 6, 8, and 28 of rhEPO treatment. EPO levels were assessed by enzyme-linked immunoabsorbent assay (ELISA) kit (R&D Systems, Minneapolis, MN, USA). Sera and plasma were obtained as described previously [42].

2.3 Immunodepletion

Sera and plasma were thawed on ice for immunodepletion by using Agilent multiple affinity removal system (MARS) kit (Agilent Technologies). The columns Human 7 (Hu7) and Human 14 (Hu14) were installed onto an Agilent 1200

Series HPLC (Agilent Technologies). In total, 40 μL of each sample were diluted fourfold in buffer A and centrifuged with 0.22 μm filters (Cellulose acetate Spin-X, Corning, NY, USA) to remove any cells and debris. After this process, the samples were immunodepleted by MARS columns 4.6 × 50 mm both Hu7 and Hu14 as recommended by the manufacturers. Low-abundance protein (LAP) and high-abundance protein (HAP) fractions were eluted in buffer A and buffer B, respectively. Subsequently, each fraction was quantified by BCA (BiCinchoninic Acid) assay (Pierce Chemical, Rockford, IL, USA) and desalted by an mRP-C18 column (Agilent Technologies) in an Agilent 1200 Series HPLC and eluted in 0.1%TFA in ACN; the reproducibility was estimated by comparing ten chromatographic peak areas per sample.

2.4 SDS-PAGE

After dilution in 2 × loading buffer (125 mM Tris, 4% SDS, 10% glycerol, 130 mM DTT, BBF in traces), 5 μg of crude, Hu7 depleted, and Hu14 depleted sera were loaded twice to see the reproducibility of immunodepletion techniques. Electrophoresis was carried out in a discontinuous buffer system with a 4% T stacking gel, pH 6.8, and a 15% T, pH 8.8 running gel. The gel was stained with SYPRO Ruby and scanned with Typhoon laser scanner 9200 (GE Healthcare) at 532 nm excitation with a 610 nm band pass emission filter. For protein identification, the band of interest was excised from gel and subjected to in situ hydrolysis.

2.5 Protein labeling

After immunodepletion, three serum samples were concentrated with vacuum centrifuge (Concentrator 5301, Eppendorf AG, Hamburg, Germany) and proteins were selectively precipitated using PlusOne 2-D Clean Up kit (GE Healthcare), to remove nonproteinaceous material, and resuspended in lysis buffer (7 M urea, 2 M thiourea, 4% CHAPS, 30 mM Tris, and 1 mM PMSF). Protein concentration was determined using PlusOne 2-D Quant kit (GE Healthcare). Briefly, 50 μg from each immunodepletion type were labeled with 400 pmol Cy5 dye, whereas the internal standard, generated by pooling together an aliquot of Hu7 and Hu14 serum, was labeled with 400 pmol Cy3 dye. The minimal labeling was performed according to the manufacturer's recommendations by incubating samples on ice in the dark for 30 min. The labeling reaction was quenched with 1 mL L-lysine 10 mM on ice for 10 min in the dark. The three samples were pooled prior to the 2-DE analysis. The ''two dyes'' protocol was adopted: the present experimental design was performed by image acquisition with a two laser scanner, Typhoon 9200, and the combination of Cy3:Cy5, due to the labeling efficiency and reliability compared with other dye combination, as described previously [44–47]. Moreover, the use of the two dyes and the manufacturer's dye/protein ratio make the dye swap unnecessary since all samples undergoing the statistical analysis had been labeled with the same dye (Cy5) and were normalized against the same internal standard (labeled with Cy3).

2.6 2-D differential gel electrophoresis

Before IEF, Cy samples were resuspended in 2 × sample buffer containing 130 mM DTT and 2% v/v IPG buffer. Individual samples (40 μg) were combined with an equal amount of internal standard; rehydratation buffer (7 M urea, 2 M thiourea, 2% CHAPS, 65 mM DTT, 0.5% IPG buffer, pH 3.5–9.5, and BBF in traces) was added to a final volume of 350 μL. Proteins from pooled samples were separated by 2-DE utilizing a 18 cm pH 3–10 nonlinear (NL) gradient IPG strips by applying the following IEF voltage steps: 200 V (2 h), 500 V (1 h), 1000 V (1 h), 2000 V (30 min), 3000 V (30 min), gradient 3000–8000 V (5 h), 8000 V until 65 000 VhT. IEF was performed using an IPGphor electrophoresis unit (GE Healthcare). At the completion of the focusing process, IEF strips were equilibrated in an SDS-reducing buffer (6 M urea, 2% SDS, 20% glycerol, 375 mM Tris-HCl, pH 8.8, 65 mM DTT) for 15 min, and then alkylated for 8 min in the same buffer containing 135 mM iodoacetamide instead of DTT. Second dimension was carried out in (20 × 25 cm), 12% T, 2.5% C, constant concentration, polyacrylamide gels at 20°C, and 15 mA per gel using the Ettan Dalt II system (GE Healthcare).

2.7 Image acquisition and analysis

CyDye-labeled gels were visualized using a Typhoon 9200 laser scanner (GE Healthcare). Excitation and emission wavelengths were chosen according to the manufacturer's recommendations (532 and 633 nm laser beams; 580 and 670 nm emission filters). Spot detection was performed using DeCyder DIA module v. 6.5 (Difference In-gel Analysis, GE Healthcare). Filters parameters were set as follows: slope 1.2, minimal area cutoff 300, and peak height 14. The DeCyder BVA module v. 6.5 (Biological Variation Analysis, GE Healthcare) was employed for inter-gel protein spot matching, whereas statistical analysis was performed using DeCyder EDA module v. 1.0 (Extended Data Analysis, GE Healthcare). Statistically significant differences were computed by Student's *t*-test, the significance level was set at $p < 0.01$. False discovery rate (FDR) was applied as multiple test correction in order to keep the overall error rate as lower as possible and only spots common to all replicates were taken into consideration.

In order to indicate how many spots have a certain abundance, normalized volumes (Cy5/Cy3) both for Hu7 and for Hu14 spots were downloaded by DeCyder and mean values calculated for each spot. Subsequently seven

normalized volume ranges were considered (0–1, 1–5, 5–10, 10–20, 20–50, 50–100, and above 100, respectively) for each immunodepletion type and the number of spots into each range was calculated and indicated in *y*-axis.

2.8 Protein identification by MS

For protein identification, semi-preparative gels were performed: gels were loaded with unlabelled Hu7 and Hu14 columns immunodepleted samples, respectively (400 μg per strip), and proteins were separated as described for analytical gels. After 2-DE, gels were stained with Deep Purple total fluorescent stain (5 mL/L) following the manufacturer's recommendations. Image acquisition was performed by Typhoon 9200 laser scanner (excitation wavelength of 532 nm and emission wavelength filter of 560 nm). Spots were gel excised by means of the Ettan spot picker robotic system (GE Healthcare) and digested with 30 μL of 5 ng/μL trypsin dissolved in 10 mM AMBIC at 37°C overnight. Released peptides underwent RP chromatography using Zip-Tip C18 micro (Millipore, Bedford, MA, USA) and eluted with 50%ACN/0.1%TFA. One microliter of peptides mixture was spotted onto the sample plate of an Ultraflex III MALDI-ToF/ToF (Bruker Daltonics) mass spectrometer; an equal volume of 10 mg/mL CHCA matrix dissolved in 70% ACN/30% 50 mM citric acid was applied and spots were air dried at room temperature. MS proceeded with an accelerating voltage of 25 kV and spectra were externally calibrated using Peptide Calibration Standard mixture; 1000 laser shots were taken per spectrum. Proteins were identified by comparing digest peaks with a computer-generated database of tryptic peptides from known proteins using in-house MASCOT 2.2, which utilizes a robust probabilistic scoring algorithm. Search was carried out by correlation of uninterpreted spectra to *Homo sapiens* entries in NCBInr 20100918 (National Center for Biotechnology Information non redundant) Database (11 823 178 sequences; 4 040 378 175 residues). With regard to MASCOT parameters, one missed cleavage per peptide was allowed, carbamidomethylation, as fixed modification, and methionine oxidation, as variable modification, no mass and p*I* constraints were set. Peptide mass tolerance was set at 30 ppm. In cases where this approach was unsuccessful, additional searches were performed using ESI MS/MS. Tandem electrospray mass spectra were recorded using a HCT Ultra mass spectrometer (Bruker Daltonics) interfaced to a MDLC (MultiDimensional Liquid Chromatography) capillary chromatograph (GE Healthcare). The samples were dissolved in 0.1% aqueous formic acid, injected onto a 0.075 × 150 mm Zorbax 300SB-C18 column (Agilent Technologies), and eluted with an ACN/0.1% formic acid gradient. The capillary voltage was set to −1600 V, and data-dependent MS/MS acquisitions were performed on precursors with charge states of 2, 3, or 4 over a survey mass range of 300–1500; the collision gas was helium. Proteins were identified by correlation of uninterpreted tandem mass spectra to *H. sapiens* entries in NCBInr 20100918, using in-house MASCOT 2.2 software. No mass and p*I* constraints were applied. One missed cleavage per peptide was allowed, and the fragment ion tolerance window was set to 0.3 Da. Carbamidomethylation of cysteine was set as fixed modification, whereas methionine oxidation was fixed as variable modification.

2.9 Matrix preparation

After immunodepletion, samples were desalted, quantitated, lyophilized, and resuspended in 0.1% TFA. Two different matrices were tested and different solutions were prepared: CHCA and DHAP (Table 1). Each solution was ready made, sonicated for 15 min, and the supernatant recovered.

As regards CHCA matrix, sample and matrix were mixed and ten replicates of 1 μL were spotted onto the AnchorChip target (600–384 target, Bruker Daltonics) and dried at room temperature.

For DHAP matrix: the sample, matrix, and 2%TFA were mixed as summarized in Table 1 and ten replicates of 1 μL of the protein solution were spotted onto the AnchorChip target and let to dry at room temperature.

2.10 MALDI profiling

Spectra were acquired in linear positive modality using an Ultraflex III mass spectrometer equipped with Smartbeam laser (frequency of 100 Hz, Bruker Daltonics), Flex Control software v. 3.3, and Flex Analysis software v.3.3 (Bruker Daltonics). Spectrometer settings were ion source 1, 25 kV; ion source 2, 23.5 kV; lens, 6.3 kV; deflection; mass suppression up to m/z 800; pulsed ion extraction, 100 ns; detector gain voltage, 1798 V; electronic gain, 50 mV/full scale; sample rate, 1 GS/s; and laser attenuator offset, 80%.

Spectra were collected using an automatic software, AutoXecute (Bruker Daltonics), whose parameters were the following: fuzzy control, off; laser power, 60%; total laser shots, 1000; random walk movement (20 shots per raster spot).

Mass spectra were analyzed by ClinProTools software v.2.2 (Bruker Daltonics) using the following spectra

Table 1. Matrices and sample preparation for MALDI profiling analysis

Matrix	Working solutions	Ratio
CHCA	0.3 μL/μL in 1:2 acetone:ethanol	1:1 (Sample/matrix)
		1:4 (Sample/matrix)
		1:10 (Sample/matrix)
DHAP	15 μg/μL in 3:1 ethanol:diammonium hydrogen citrate	1:1:1 (2% TFA:sample:matrix)
		2:2:1 (2% TFA: sample:matrix)
		1:1:2 (2% TFA: sample:matrix)

preparation parameters: 800 resolution, Top Hat Baseline, 10% minimal baseline width, Savitsky–Golay smoothing. ClinProTools' statistics was performed by Wilcoxon's *t*-test (significance level for *p*-value <0.05) through which a list of peaks was generated. The peaks were sorted along the statistical differences between selected classes (e.g. healthy controls and drug treatment) and are named ''best separating'' peaks.

3 Results and discussion

3.1 Immunodepletion

The choice of the immunodepletion strategy and MS conditions represent an essential step required for each test based on MALDI profiling. The methodological setup for rhEPO serum profiling, the efficacy and reproducibility of two commercially available columns developed for human serum immunodepletion, named MARS Hu7 and Hu14, derivatized with 6 and 13 antibodies for the most abundant proteins, was assessed. The MARS Hu7 column permits the depletion of albumin, IgG, IgA, transferrin, haptoglobin, antitrypsin, whereas MARS Hu14 column enables the removal of the same proteins plus α-2-macroglobulin, α-1-acid glycoprotein, IgM, apolipoprotein AI and AII, C3 complement, and transthyretin. The reproducibility was assessed by ten serial injections of the same serum sample and is shown in Supporting Information Fig. 1S. The protein contents of low-abundant fractions from Hu7 and Hu14 were 15.3% (SD = ±1.3) and 6.4% (SD = ±1.1), respectively, in agreement with Bjorhall et al. [17] and concentration differences correspond to the assumed amount of the seven depleted proteins by Hu14 [48]. Column specificity is shown in Fig. 1. Crude serum, high-abundance fractions (HAP Hu7, HAP Hu14) and low-abundant fractions (LAP Hu7, LAP Hu14) from three serum samples, pooled after Hu7 and Hu14 immunodepletion, were analyzed in 15% T SDS-polyacrylamide. Proteins were visualized by SYPRO Ruby fluorescent staining. A higher number of bands are visualized using Hu14 immunodepletion, indicating a reduction of the dynamic range. The attention was focused on the low-abundant fraction which contains proteins of clinical interest [49]. To accurately define qualitatively and quantitatively the effects of immunodepletion on serum proteome, a 2-D differential gel electrophoresis (DIGE) analysis was carried out, being the sensitivity of this methodology in the order of picograms [50]. In total, 40 μg of both Hu7 and Hu14 low-abundant fractions from three pooled samples were labeled with Cy5, together with the internal standard, labeled with Cy3 and separated utilizing a 18 cm, pH 3–10 NL gradient, as first dimension. Each sample was analyzed in triplicate and image analysis was performed by DeCyder software. Overall, 1419 spots were matched per gel; among them 128 spots were differentially changed (*t*-test, $p<0.01$) in Hu14 versus Hu7 sera.

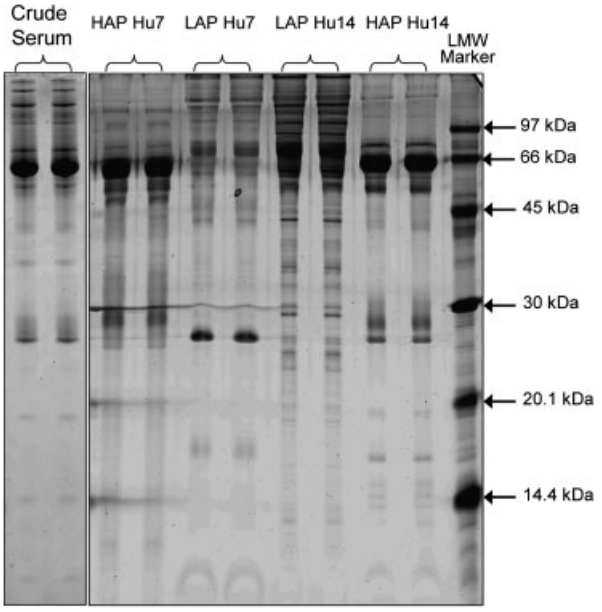

Figure 1. Representative SDS-PAGE of total serum, MARS Hu7 high-abundance (HAP Hu7), MARS Hu7 low-abundance (LAP Hu7), MARS Hu14 low-abundance (LAP Hu14), and MARS Hu14 high-abundance (HAP Hu14) fractions. Five micrograms of each sample were loaded per lane and electrophoresis was carried out in a discontinuous buffer with a 4% T, 2.5% C stacking gel, pH 6.8, and a 15% T, 2.5% C, pH 8.8 running gel. The gel was stained with SYPRO Ruby and scanned at 532 nm excitation with a 610 nm band pass emission filter with Typhoon laser scanner.

Figure 2A shows the differences in spot distribution with same abundance calculated by averaged normalized volumes Cy5/Cy3, respectively, for Hu7 and Hu14 immunodepleted samples. Hu7 gels contain ∼12% more spots in the range 0–1 compared with Hu14. On the contrary, in Hu14 gels, a general increment in spot distribution, particularly in the ranges 1–5 and 5–10, was observed, indicating that the decrement of the dynamic range was associated with an increment in spot number with higher values of normalized volumes. Out of 128 spots differentially expressed, 96 were identified by MS. The identified proteins together with the average ratio, Student's *t*-test *p*-value, UniProt KB Entries, theoretical p*I*, and molecular weights are listed in Tables 2 and 3 for Hu7 and Hu14 gels, respectively (Supporting Information Tables 1S and 2S for supporting data related to MS identifications). Among differentially changed spots, 16 were strongly decreased in Hu14 gels with respect to Hu7 as shown in Fig. 2B. In particular, proteins removed by Hu14 column were identified: four isoforms of complement component C3 (average ratios of −74.75, −2.08, −86.07, and −22.34, respectively); six isoforms of α-2-macroglobulin (average ratios equal to –1.5, −1.16, −1.16, −1.36, −1.37, and −1.42 respectively); α-1-acid glycoprotein 1 (average ratio, –16.64); two isoforms of apolipoprotein AI (−27.74 and −28.64, respectively) and three isoforms of transthyretin (−12.31, −57.88, and −435.39, respectively). As far as concerned α-2-macro-

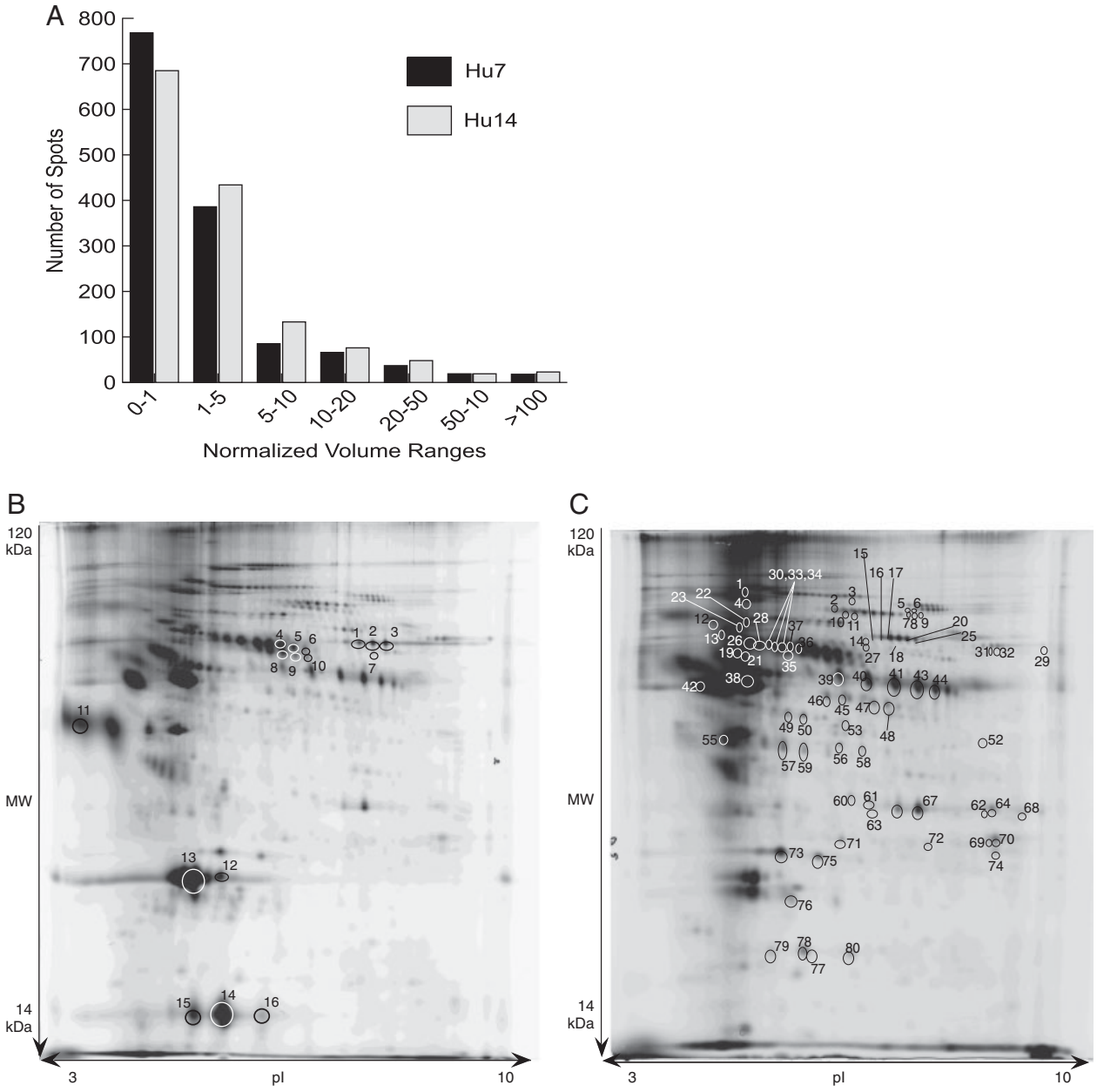

Figure 2. (A) The histogram distribution of spots with a certain abundance both after Hu7 and Hu14 depletion. The ranges were calculated as averaged normalized volumes obtained from the BVA module of DeCyder software. (B) A representative 2-D DIGE gel image of Cy5-labeled MARS Hu7-depleted serum in which less abundant proteins in Hu14 maps respect to Hu7 are identified and indicated by circles (reference to Table 2). (C) A representative 2-D DIGE gel image of Cy5-labeled MARS Hu14-depleted serum in which the identified proteins, more abundant in Hu14 maps respect to Hu7, are indicated (Table 3). In both experiments, 40 μg of protein mixture was separated in pH 3–10 NL IPG strips in the first dimension until 65 000 VhT, followed by a SDS gel (12% T, 2.5% C) carried out at 15 mA/gel at 20°C, O/N. Images were acquired by Typhoon laser scanner, excitation and emission wavelengths were chosen according to the manufacturer's recommendations (633 nm laser beam and 670 nm emission filter).

globulin, the slightly decreased spots could be associated to protein fragments of the intact protein, with low affinity for the antibody bound to columns. The intact protein is absent in our 2-D map. In addition, a clear increment of proteins usually defined ''scarcely abundant'' was observed in Hu14 gels respect to Hu7 (Fig. 2C). In particular, eleven spots with average ratio >3 were detected. The enriched proteins in Hu14 sample were two isoforms of plasma glutathione peroxidase (average ratios, 32.77 and 3.47, respectively), retinol-binding protein 4 (average ratio, 18.59), apolipoprotein E precursor (average ratio, 7.62), light chain of factor I (average ratio, 6.55), and six isoforms of complement factor B (average ratios equal to 6.03, 5.85, 4.71, 4.3, 3.77, and 3.23, respectively). Besides, proteins such as kallikrein (two

Table 2. Less abundant proteins in Hu14-depleted sera compared with Hu7 depleted sera

Spot number	*t*-Test *p*-value	Average ratio V_R/V_C (fold change)	Name	Swiss-Prot accession number	Theoretical p*I*	Theoretical MW (Da)
1	0.000109	−22.34	Complement C3 β chain	P01024	6.82	71 316.61
2	2.15E−05	−74.45	Complement C3 β chain	P01024	6.82	71 316.61
3	2.85E−04	−86.07	Complement C3 β chain	P01024	6.82	71 316.61
4	1.66E−03	−1.16	α-2-Macroglobulin	P01023	5.98	160 809.88
5	1.28E−03	−1.37	α-2-Macroglobulin	P01023	5.98	160 809.88
6	1.02E−03	−1.42	α-2-Macroglobulin	P01023	5.98	160 809.88
7	1.87E−04	−2.08	Complement C3 β chain	P01024	6.82	71 316.61
8	4.31E−03	−1.16	α-2-Macroglobulin	P01023	5.98	160 809.88
9	9.25E−05	−1.36	α-2-Macroglobulin	P01023	5.98	160 809.88
10	7.05E−03	−1.50	α-2-Macroglobulin	P01023	5.98	160 809.88
11	4.79E−04	−16.64	α-1-acid Glycoprotein 1	P02763	5.00	21 560.12
12	3.17E−06	−28.64	Apolipoprotein AI	P02647	5.27	28 078.62
13	2.63E−06	−27.74	Apolipoprotein AI	P02647	5.27	28 078.62
14	4.27E−06	−435.39	Transthyretin precursor	P02766	5.52	15 887.03
15	1.95E−03	−57.88	Transthyretin precursor	P02766	5.52	15 887.03
16	8.27E−04	−12.31	Transthyretin precursor	P02766	5.52	15 887.03

Spot number refers to Fig. 2B, Uni-Prot KB entries, name, theoretical p*I*, and molecular weights are indicated. V_R/V_C indicates the value derived from the normalized spot volume standardized against the intragel standard provided by DeCyder software analysis.

isoforms 1.28-fold and 1.48-fold increased, respectively) with a blood concentration at the picomolar level were identified in Hu14 but not in Hu7 samples. Same spots were detectable by DeCyder software but were undetectable by MS presumably because their abundance in gels was below the detection limit of the mass spectrometer after gel picking and in situ digestion. Finally, this analysis highlights secreted proteins as cytoplasmatic peroxiredoxin 2 (average ratio, 1.4) and carbonic anhydrase 1 (average ratio, 1.33). Immunodepleted serum after Hu14 indicates a decrement of at least one order of magnitude in the dynamic range which allows to identify proteins at the picomolar level.

3.2 MALDI profiling

The MALDI profiling is based on the assessment of differences in peak intensities among two or more groups. The choice of the matrix represents a crucial step and a number of compounds have been developed for different applications. Due to their peculiarities, CHCA and DHAP matrices have been chosen for the proposed experimental setup for human serum profiling.

Hu7 and Hu14 immunodepleted sera were analyzed using CHCA and DHAP and an AnchorChip target was adopted to increment the sensitivity, as suggested by Leung and Pitts [51]. After immunodepletion, serum samples were lyophilized and resuspended in 0.1%TFA at 1 μg/μL concentration. Spectra reproducibility was assessed by randomly spotting samples to the target, in ten replicates, to reduce the variability related to a particular position.

Concerning CHCA, 1 μL of each sample was loaded onto the MALDI target adopting different sample/matrix ratios and the best conditions for serum analysis appeared to be the matrix ratio 1:4 and 1:10. After Hu7 depletion, 111 and 140 peaks were detected, respectively, with an average CV% of 15.4 for 1:4 ratio and 16.5 for 1:10 ratio, whereas Hu14 depletion provided 120 and 145 peaks for each dilution with an average CV% of 15 and 13, respectively. Hu7 depletion gives an increased number of peaks in 1:10 ratio but with a higher CV% value. Conversely, the sample, depleted using the Hu14 column, shows an increase in both sensitivity and reproducibility. Comparing Hu7 and Hu14 profiles, a peak at m/z 14 000 present in the former disappears in the latter, suggesting that this signal probably represents one of the proteins removed by Hu14 column (Fig. 3A and B). This suggests that CHCA is a suitable matrix for analyzing profiles up to m/z 15 000 but not above this value. By analyzing serum, we expect to find a number of small proteins and peptides released in the blood stream after rhEPO treatment over m/z 15 000. To increase the range of peak detection DHAP with different dilutions, different pH and solvent ratios were investigated. Regarding Hu7-immunodepleted samples, among different %TFA:sample:matrix ratios, the most promising appeared at a ratio of 2:2:1 which shows good sensitivity in the range of m/z 1000–32 000 (a total of 214 peaks were detected with a CV% of 17.4; Supporting Information Table 3S), whereas the ratio 1:1:2 provided a good quality only beyond m/z 5000 (Supporting Information Fig. 2S). Matrix dilution ratios were optimized in parallel for Hu14 immunodepleted sera and the selected conditions were 1:1:1 2% TFA:sample:matrix ratio by which 210 peaks were detected with a CV% of 18.4 as summarized in Supporting Information Table 4S. The differences in peak patterns, related to the difference in the dynamic range of the applied sample (Hu7 and Hu14 depleted samples), are shown in Fig. 3C and D (for the enlarged spectra, see Supporting Information

Table 3. More abundant proteins in Hu14-depleted sera compared with Hu7-depleted sera

Spot number	*t*-Test *p*-value	Average ratio V_R/V_C (fold change)	Name	Swiss-Prot accession number	Theoretical p*I*	Theoretical MW (Da)
1	4.50E−03	1.27	Ceruloplasmin	Q1L857	5.43	115 471.66
2	2.34E−02	1.10	Complement component C7 precursor	P10643	6.09	93 518.24
3	2.37E−03	1.11	Factor H	P08603	6.12	137 052.59
4	8.62E−03	1.28	Inter-α-trypsin inhibitor heavy chain H4 isoform 2 precursor	B7ZKJ8	6.43	103 880.97
5	5.07E−04	1.66	Coagulation factor XII	P00748	8.04	67 792.09
6	4.49E−03	1.35	Coagulation factor XII	P00748	8.04	67 792.09
7	3.05E−04	1.55	Coagulation factor XII	P00748	8.04	67 792.09
8	2.26E−04	1.39	Coagulation factor XII	P00748	8.04	67 792.09
9	1.08E−03	1.28	Plasma kallikrein precursor	P03952	8.60	71 369.69
10	1.96E−04	1.25	Chain A. Human complement factor B	P00751	6.66	83 000.80
11	5.27E−04	1.25	Chain A. Human complement factor B	P00751	6.66	83 000.80
12	5.82E−03	1.08	Plasma protease C1 inhibitor precursor variant	P05155	6.09	55 154.19
13	3.22E−02	1.14	Vitronectin precursor	P04004	5.55	54 305.59
14	3.05E−03	2.10	Factor H	P08603	6.12	137 052.59
15	2.33E−04	4.71	Complement factor B	P00751	6.66	83 000.80
16	1.70E−04	5.85	Complement factor B	P00751	6.66	83 000.80
17	1.46E−04	6.03	Complement factor B	P00751	6.66	83 000.80
18	1.29E−05	4.30	Complement factor B	P00751	6.66	83 000.80
19	5.08E−03	1.39	α-1-B-glycoprotein	P04217	5.63	51 921.66
20	9.70E−06	3.77	Complement factor B	P00751	6.66	83 000.80
21	3.86E−03	1.45	Angiotensinogen	P01019	5.60	49 761.11
22	1.80E−03	1.45	Complement C1r subcomponent precursor	P00736	5.76	78 213.16
23	4.90E−02	1.28	Insulin-like growth factor binding protein. Acid labile subunit	Q8TAY0	6.33	66 067.07
24	2.39E−05	3.23	Complement factor B	P00751	6.66	83 000.80
25	7.89E−04	2.78	Complement factor B	P00751	6.66	83 000.80
26	2.45E−04	1.40	Hemopexin precursor	P02790	6.43	49 295.43
27	6.24E−03	1.35	Factor H	P08603	6.12	137 052.59
28	1.09E−04	1.52	Hemopexin precursor	P02790	6.43	49 295.43
29	2.16E−03	1.37	C4A protein	A6H8M8	6.70	187 703.64
30	1.04E−04	1.43	Hemopexin precursor	P02790	6.43	49 295.43
31	1.39E−03	1.31	C4A protein	A6H8M8	6.70	187 703.64
32	4.32E−03	1.28	C4A protein	A6H8M8	6.70	187 703.64
33	1.72E−03	1.23	Hemopexin precursor	P02790	6.43	49 295.43
34	9.83E−03	1.08	Gelsolin isoform a precursor	P06396	5.72	82 959.11
35	6.04E−05	1.87	Hemopexin precursor	P02790	6.43	49 295.43
36	7.89E−03	1.13	Gelsolin isoform a precursor	P06396	5.72	82 959.11
37	4.16E−04	1.24	Hemopexin precursor	P02790	6.43	49 295.43
38	3.62E−03	1.30	Vitamin D-binding protein/group-specific component	P02774	5.40	52 963.65
39	1.45E−04	1.40	β-2-Glycoprotein 1 precursor	P02749	8.30	38 298.00
40	1.28E−04	1.38	β-2-Glycoprotein 1 precursor	P02749	8.30	38 298.00
41	1.39E−03	1.31	β-2-Glycoprotein 1 precursor	P02749	8.30	38 298.00
42	7.29E−02	1.15	Complement C4B chain	P0C0L5	8.69	71 678.89
43	1.87E−04	1.25	β-2-Glycoprotein 1 precursor	P02749	8.30	38 298.00
44	8.27E−04	1.15	β-2-Glycoprotein 1 precursor	P02749	8.30	38 298.00
45	1.02E−03	1.34	CFI protein	Q8WW88	8.49	42 432.18
46	7.83E−04	1.24	CFI protein	Q8WW88	8.49	42 432.18
47	3.60E−04	1.25	CFI protein	Q8WW88	8.49	42 432.18
48	1.24E−03	1.21	CFI protein	Q8WW88	8.49	42 432.18
49	1.02E−03	1.24	Pigment epithelial-differentiating factor	P36955	5.90	44 387.80
50	2.32E−04	1.12	Complement factor H-related 1	Q03591	7.10	35 738.20
51	2.29E−04	1.12	Pigment epithelial-differentiating factor	P36955	5.90	44 387.80
52	1.12E−03	1.48	Plasma kallikrein B1 precursor	P03952	8.60	71 369.69

Table 3. Continued

Spot number	*t*-Test *p*-value	Average ratio V_R/V_C (fold change)	Name	Swiss-Prot accession number	Theoretical p*I*	Theoretical MW (Da)
53	5.76E−03	1.23	Complement factor H-related 1	Q03591	7.10	35 738.20
54	1.95E−02	1.14	Complement factor H-related 1	Q03591	7.10	35 738.20
55	3.74E−03	2.74	Apolipoprotein J precursor	P10909	5.89	50 062.56
56	9.50E−04	2.77	Complement factor H-related 1	Q03591	7.10	35 738.20
57	8.91E−05	7.62	Apolipoprotein E precursor	P02649	5.52	34 236.68
58	6.60E−04	1.93	Complement factor H-related 1	Q03591	7.10	35 738.20
59	8.85E−04	3.47	Plasma glutathione peroxidase	P22352	8.26	25 402.30
60	3.33E−03	1.17	Ficolin-3 isoform 1 precursor	O75636	6.20	32 902.98
61	0.0107	1.13	Ficolin-3 isoform 1 precursor	O75636	6.20	32 902.98
62	3.07E−05	1.89	C4B3	Q6U2L1	5.78	47 454.07
63	2.33E−04	1.25	cDNA FLJ55146. Highly similar to complement C4-B	B4DDH0	6.12	57 513.06
64	2.45E−04	1.94	C1q B-chain precursor	P02746	8.83	26 721.76
65	0.0231	1.26	Complement component 4A	B2RUT6	6.59	192 776.47
66	0.0475	1.16	Complement component 4A	B2RUT6	6.59	192 776.47
67	4.58E−03	1.24	cDNA FLJ55146. Highly similar to complement C4-B	B4DDH0	6.12	57 513.06
68	1.34E−04	2.79	C1q B-chain precursor	P02746	8.83	26 721.76
69	1.23E−03	1.38	C1q B-chain precursor	P02746	8.83	26 721.76
70	8.85E−04	1.41	C1q B-chain precursor	P02746	8.83	26 721.76
71	9.98E−02	1.11	Complement Factor H-related Protein 2	P36980	5.80	28 738.37
72	2.07E−03	1.33	Carbonic anhydrase 1	P00915	6.63	28 739.02
73	6.10E−05	1.62	Serum amyloid P component precursor	P02743	6.10	25 387.13
74	7.83E−04	1.42	Chain B. Globular head of the complement system protein C1q	P02746	8.85	23 741.92
75	3.58E−04	1.35	Serum amyloid P component precursor	P02743	6.10	25 387.13
76	1.44E−02	1.40	Peroxiredoxin-2 isoform a	P32119	5.66	21 891.92
77	1.72E−01	1.16	Tetranectin precursor	P05452	5.52	22 536.81
78	2.76E−04	32.77	Plasma glutathione peroxidase	P22352	8.26	25 402.30
79	4.38E−04	6.55	Light chain of factor I	Q6LAM0	6.24	27 592.38
80	1.44E−03	18.59	Retinol binding protein 4 plasma	P02753	5.76	23 010.01

V_R/V_C indicates the value derived from the normalized spot volume standardized against the intragel standard provided by DeCyder software analysis. Spot number refers to Fig. 2C. Uni-Prot KB entries name, theoretical p*I*, and molecular weights are indicated.

Figs. 3S and 4S) where it can be noticed that peaks at m/z 28 000 and at m/z 14 000 values (indicated by arrows) are present in Hu7 sample but absent in Hu14-immunodepleted sample. In addition, by comparing profiling from the two matrices, a peak at m/z 14 000 value was visualized in both CHCA and DHAP matrices. This will presumably represent the double-charged specie of an m/z 28 000 peak which is common to both, low-abundant fractions (LAP) and high-abundant fractions (HAP) of Hu7 and Hu14, respectively (Fig. 1). This peak corresponds to apolipoprotein AI (Uni-Prot KB Entry P02647, MASCOT score 176, coverage 42%) removed by the Hu14 column and identified after 1-D SDS PAGE followed by MS. Figure 4 shows Hu14 profiling by adopting CHCA and DHAP matrices, respectively. DHAP allows the analysis of a wider m/z range and provides spectra with a lower background to noise ratio, making it the selected matrix for our purposes.

In clinical practice, the employment of different specimens (whole blood, serum, or plasma) is strictly related to the nature of the test; in particular, plasma is utilized when coagulation factors are of interest. To select the appropriate specimen for rhEPO monitoring, the efficacy of the selected conditions was also evaluated in plasma. Plasma profiling was conducted adopting DHAP matrix (ratio, 1:1:1) as shown in Fig. 5. Signals up to m/z 20 000 were detected, and the profile includes 161 peaks with a CV% of 18.1 but with lower intensity. The presence of high-abundant coagulation and fibrinolytic components, which hamper the identification of less abundant species, suggests that serum is the specimen of choice for applying this protocol.

3.3 The case of rhEPO treatment

The above-described experimental setup was finalized to the study of a specific condition: the evaluation of changes in human serum before and after a low dose (65 IU/Kg) of rhEPO. Serum samples were collected from ten healthy young male volunteers, carefully selected, and well-char-

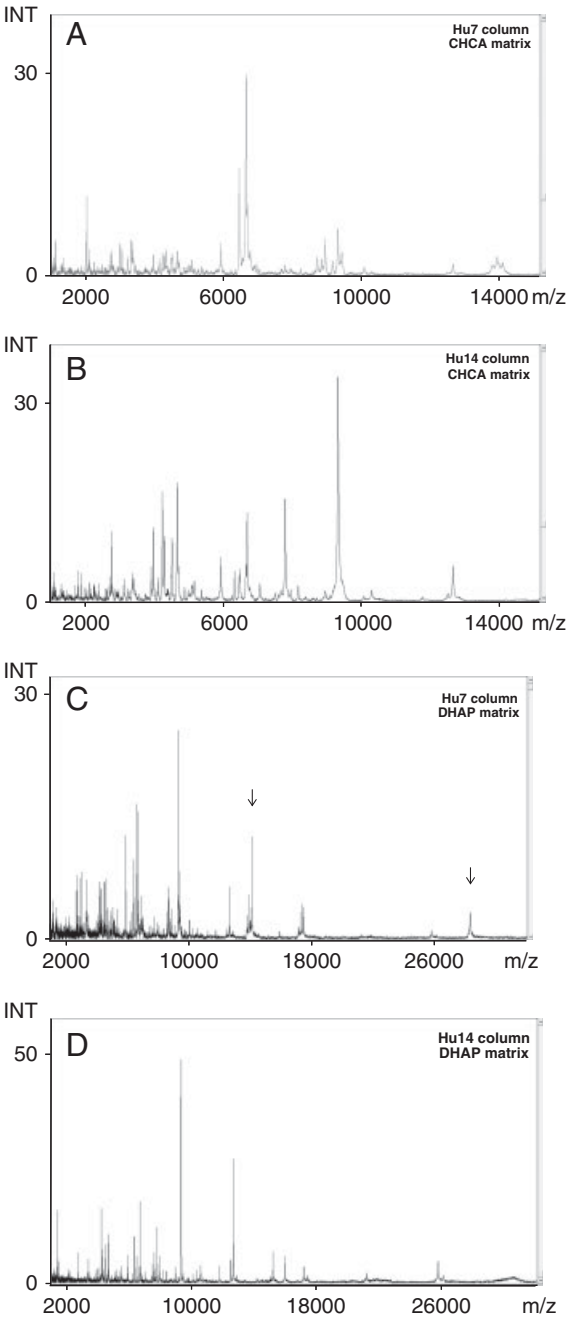

Figure 3. ClinProTools average spectra for MARS Hu7 (A) and MARS Hu14 (B) column immunodepleted serum analyzed with CHCA matrix. Spectra were acquired in linear mode in the *m/z* range of 1000–15 000. (C and D) ClinProTools average spectra for MARS Hu7 and MARS Hu14 column-immunodepleted serum, respectively, analyzed with DHAP matrix. Spectra were acquired in linear mode in the *m/z* range of 1000–32 000. In (C), arrows indicate the peaks at *m/z* 14 000 and 28 000 that could refer to single- and double-charged species of apolipoprotein AI, respectively. In all cases, each sample was spotted random onto the AnchorChip target in ten replicates.

acterized subjects. Characteristics of the subjects have been described previously [42]. By profiling these samples, we expected to detect the differences related to changes induced

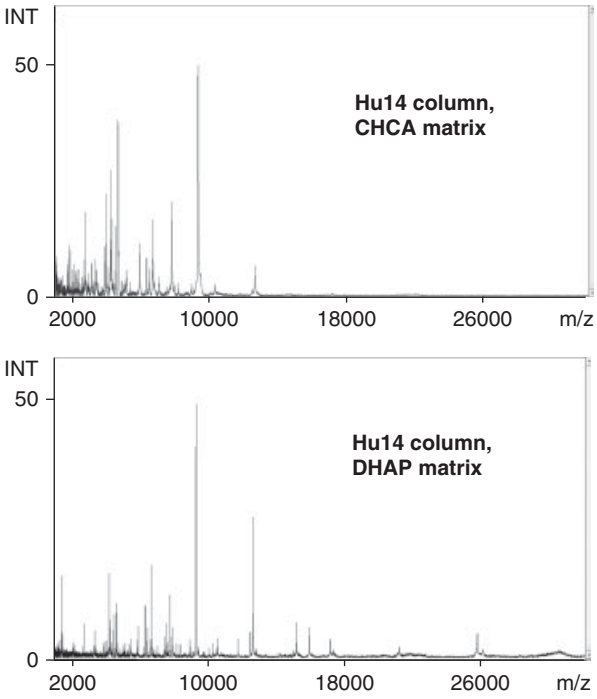

Figure 4. ClinProTools average spectra for MARS Hu14-immunodepleted serum analyzed both with CHCA (1:10 sample/matrix ratio; upper panel) and DHAP matrices (2:2:1, 2 %TFA/sample/matrix ratio; lower panel). Each sample was randomly spotted onto the AnchorChip target in ten replicates and spectra were acquired in the *m/z* range of 1000–32 000.

by increased erythropoiesis, hematocrit, hemoglobin, and iron mobilization, and to propose a new method for monitoring rhEPO treatment that could be useful for both clinical purposes and antidoping tests. The time course of plasma EPO levels (Supporting Information Fig. 5S) monitored as described previously [42], increased up to three times in plasma after 6 days of treatment; accordingly, a similar increment was expected in serum and thus we focused our attention on samples at day 0 (control samples) and at day 6, in which EPO reached the maximal concentration. Both columns, Hu7 and Hu14, were adopted to verify the effects on the dynamic range of samples treated with rhEPO, whereas DHAP was the matrix of choice.

Low-abundant fractions from Hu7-immunodepleted sera were loaded onto a MALDI AnchorChip target as described previously. Twenty-three differentially changed peaks (Wilcoxon rank sum test p-value <0.05) in m/z range 1000–18 000 were obtained and the average sum of spectra from control and treated sera is shown in Fig. 6A together with a closeup of a selection of most significant peaks (Wilcoxon rank sum test p-value <0.05) differentiating the two cohorts. Unsupervised principal component analysis (PCA) was unable to discriminate between treated and untreated sera (Fig. 6B): the score plots did not reveal a clustering of samples according to the rhEPO treatment. By utilizing MARS Hu14 column, the LAP fractions were also analyzed with 1:1:1 2% TFA:sample:matrix in the m/z range

1000–32 000. By comparing treated samples versus controls, 186 best separating peaks were detected (Wilcoxon rank sum test p-value <0.05). The average spectra from controls and treated sera are shown in Fig. 7A, the closeup refers to the most significant peaks with a p-value <0.000001. In this case, unsupervised PCA could discriminate between classes. In Fig. 7B, the scores plots indicate a sample's clusterization, suggesting that the selected conditions adopted for sample preparation and the appropriate matrix and dilutions allow to discriminate new peptides associated to rhEPO treatment, opening new perspectives in the use of MALDI profiling in monitoring rhEPO.

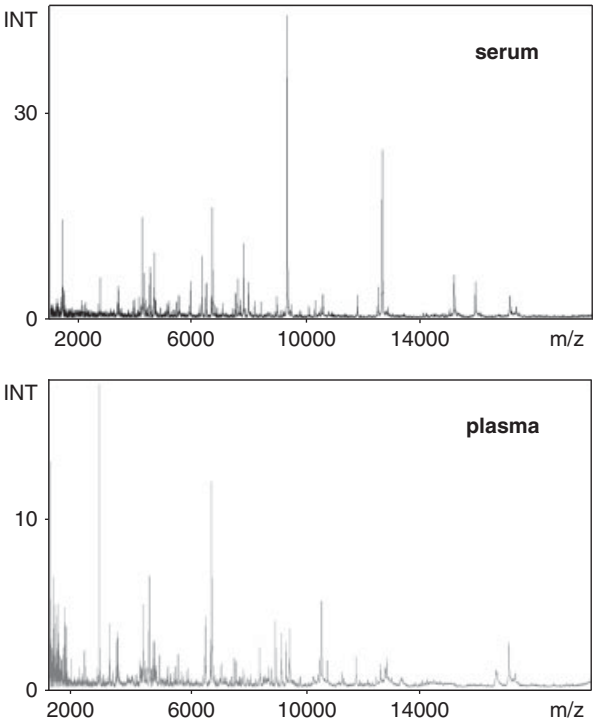

Figure 5. ClinProTools average spectra for serum (upper panel) and plasma (lower panel) depleted with MARS Hu14 column and analyzed with DHAP matrix (2:2:1, 2%TFA/sample/matrix ratio). Each sample was spotted random onto the AnchorChip target in ten replicates and spectra were acquired in linear mode in the *m/z* range of 1000–20 000.

4 Concluding remarks

The effect of serum dynamic range reduction was assessed in control serum samples, by defining parameters crucial for the identification of low-abundant species and for the quality of MALDI profiling analysis. After comparing the enrichment provided by the two columns, we conclude that the use of Hu14 allows to enrich less abundant fraction (80 proteins more represented in LAP), suggesting that immunodepletion by adopting Hu14 is an efficient and effective reproducible tool for improving the use of biological fluids for clusterizing samples, for monitoring disease progression and therapies. In addition, the identification of secreted proteins (i.e. peroxiredoxin 2 and carbonic anhydrase 1) further supports the use of MALDI profiling for monitoring pathological states that involve release of specific proteins (largely expressed in organs or tissues like heart, muscles, or tumors) in the bloodstream, thus broadening the possibility to identify new biomarkers or to adopt this technology for profiling changes induced by a specific disease. Moreover, the identification of proteins present at picomolar level, such as kallikrein, opens new opportunities in the detection of signal molecules relevant for clinical diagnosis but undetectable without the removal of the most abundant species. All these remarks, when translated in the investigation of proteins and peptides for monitoring rhEPO treatment in human subjects, show the efficacy of the proposed setup as supported by the

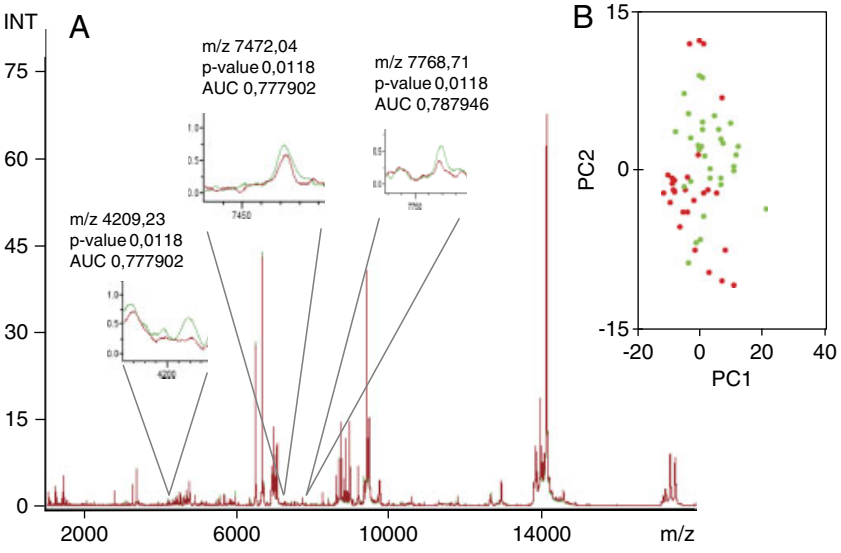

Figure 6. (A) The average spectra related to MARS Hu7 LAP fractions from control (red) and rhEPO-treated subjects (green). Immunodepleted sera were loaded onto the MALDI AnchorChip target (2%TFA:sample:DHAP in the ratio of 2:2:1) and spectra were analyzed by ClinProTools. Twenty-three best-separating peaks were observed (Wilcoxon rank sum test p-value <0.05) in the *m/z* range of 1000–18 000 and three out of them are shown as closeup. (B) The unsupervised PCA which is unable to distinguish between groups of the untreated (red) and treated (green) sera.

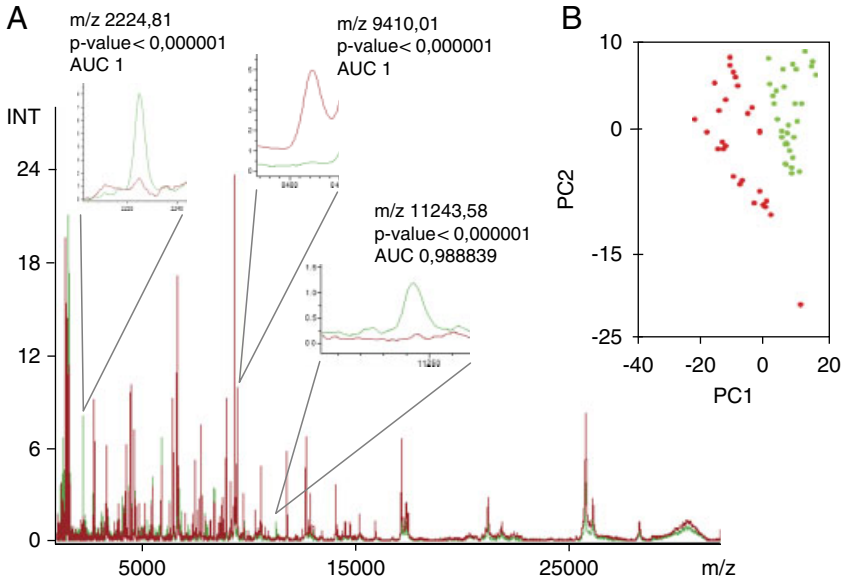

Figure 7. (A) The average spectra related to MARS Hu14 LAP fractions from control (red) and rhEPO-treated subjects (green). Immunodepleted sera were loaded onto the MALDI AnchorChip target (2% TFA:sample:DHAP in the ratio of 1:1:1) and spectra were analyzed by ClinProTools. In all, 186 best-separating peaks were observed (Wilcoxon rank sum test *p*-value <0.05) in the *m/z* range of 1000–32 000 and three out of them are shown as closeup. (B) The unsupervised PCA is able to discriminate between untreated (red) and treated (green) sera.

unsupervised PCA. It goes without saying that a careful subject selection and the control of physiological and pathological conditions represent a fundamental issue to put forward the implementation of MALDI profiling for rhEPO monitoring in clinical practice. For a prediction model and validation, a larger number of samples are required; nevertheless, the proposed setup fulfils the preconditions for performing clinical investigations adopting high-throughput technologies. In conclusion, the present results indicate that the combination of Hu14 column and DHAP matrix by increasing data quality represents an appropriate approach for rhEPO serum profiling by MALDI.

This work has been funded from: Italian Ministry of University and Scientific Research (Grant: FIRB RBRNO7BMCT to C. G.), Italian Institute of Technologies (Grant: SEED-IPG-CHIP 21531 to C. G.), EU (Grant: BIO-NMD 241665 to C. G.), PRIN to C. G., and antidoping Denmark to C. L.

The authors have declared no conflict of interest.

5 References

[1] Beretta, L., *Nat. Methods* 2007, *4*, 785–786.

[2] Omenn, G. S., *Proteomics* 2006, *6*, 5662–5673.

[3] Petricoin, E. F., Ardekani, A. M., Hitt, B. A., Levine, P. J., Fusaro, V. A., Steinberg, S. M., Mills, G. B., Simone, C., Fishman, D. A., Kohn, E. C., Liotta, L. A., *Lancet* 2002, *359*, 572–577.

[4] Tirumalai, R. S., Chan, K. C., Prieto, D. A., Issaq, H. J., Conrads, T. P., Veenstra, T. D., *Mol. Cell. Proteomics* 2003, *2*, 1096–1103.

[5] Liotta, L. A., Petricoin, E. F., *J. Clin. Invest.* 2006, *116*, 26–30.

[6] Espina, V., Dettloff, K. A., Cowherd, S., Petricoin, E. F., 3rd, Liotta, L. A., *Expert Opin. Biol. Ther.* 2004, *4*, 83–93.

[7] Fujita, N., Nakanishi, M., Mukai, J., Naito, Y., Ichida, T., Kaito, M., Yoshikawa, T., Takei, Y., *Mol. Med.* 2011, *17*, 70–78.

[8] Sreseli, R. T., Binder, H., Kuhn, M., Digel, W., Veelken, H., Sienel, W., Passlick, B., Schumacher, M., Martens, U. M., Zimmerman, S., *Oncol. Rep.* 2010, *24*, 263–270.

[9] Villanueva, J., Philip, J., Entenberg, D., Chaparro, C. A., Tanwar, M. K., Holland, E. C., Tempst, P., *Anal. Chem.* 2004, *76*, 1560–1570.

[10] Diamandis, E. P., *Clin. Chem.* 2003, *49*, 1272–1275.

[11] Anderson, N. L., Anderson, N. G., *Mol. Cell. Proteomics* 2002, *1*, 845–867.

[12] Gramolini, A. O., Kislinger, T., Alikhani-Koopaei, R., Fong, V., Thompson, N. J., Isserlin, R., Sharma, P. , Oudit, G. Y., Trivieri, M. G., Fagan, A., Kannan, A., Higgins, D. G., Huedig, H., Hess, G., Arab, S., Seidman, J. G., Seidman, C. E., Frey, B., Perry, M., Backx, P. H., Liu, P. P., MacLennan, D. H., Emili, A., *Mol. Cell. Proteomics* 2008, *7*, 519–533.

[13] Gramolini, A. O., Peterman, S. M., Kislinger, T., *Clin. Pharmacol. Ther.* 2008, *83*, 758–760.

[14] Vergara, D., Chiriaco, F., Acierno, R., Maffia, M., *Proteomics* 2008, *8*, 2045–2051.

[15] Whiteaker, J. R., Zhang, H., Zhao, L., Wang, P., Kelly-Spratt, K. S., Ivey, R. G., Piening, B. D. et al., *J. Proteome Res.* 2007, *6*, 3962–3975.

[16] Georgiou, H. M., Rice, G. E., Baker, M. S., *Proteomics* 2001, *1*, 1503–1506.

[17] Bjorhall, K., Miliotis, T., Davidsson, P., *Proteomics* 2005, *5*, 307–317.

[18] Chromy, B. A., Gonzales, A. D., Perkins, J., Choi, M. W., Corzett, M. H., Chang, B. C., Corzett, C. H. , McCutchen-Maloney, S. L., *J. Proteome Res.* 2004, *3*, 1120–1127.

[19] Luque-Garcia, J. L., Neubert, T. A., *J. Chromatogr. A* 2007, *1153*, 259–276.

[20] Ramstrom, M., Hagman, C., Mitchell, J. K., Derrick, P. J., Hakansson, P., Bergquist, J., *J. Proteome Res.* 2005, *4*, 410–416.

[21] Zhang, R., Barker, L., Pinchev, D., Marshall, J., Rasamoelisolo, M., Smith, C., Kupchak, P., Kireeva, I., Ingretta, L., Jackowski, G., *Proteomics* 2004, *4*, 244–256.

[22] Freeman, T., Smith, J., *Biochem. J.* 1970, *118*, 869–873.

[23] Freed, G. L., Cazares, L. H., Fichandler, C. E., Fuller, T. W., Sawyer, C. A., Stack, B. C., Jr, Schraff, S. et al., *Laryngoscope* 2008, *118*, 61–68.

[24] Wong, M. Y., Yu, K. O., Poon, T. C., Ang, I. L., Law, M. K., Chan, K. Y., Ng, E. W. , Ngai, S. M., Sung, J. J., Chan, H. L., *Electrophoresis* 2010, *31*, 1721–1730.

[25] Fertin, M., Burdese, J., Beseme, O., Amouyel,P., Bauters, C., Pinet, F., *J. Proteomics* 2010, *74*, 420–430.

[26] Bigbee, W., Zeng, X., Hood,B. L., Sun, M., Conrads, T., Day, R. S., Weissfeld, J. L., Siegfried, J. M., Bigbee, W. L., *J. Proteome Res.* 2010, *9*, 6440–6449.

[27] Liu, T., Qian, W. J., Strittmatter, E. F., Camp, D. G., 2nd, Anderson, G. A., Thrall, B. D., Smith, R. D., *Anal. Chem.* 2004, *76*, 5345–5353.

[28] Zhang, H., Li, X. J., Martin, D. B., Aebersold, R., *Nat. Biotechnol.* 2003, *21*, 660–666.

[29] Zhang, H., Yi, E. C., Li, X. J., Mallick, P., Kelly-Spratt, K. S., Masselon, C. D., Camp, D. G., 2nd, Smith, R. D., Kemp, C. J., Aebersold, R., *Mol. Cell. Proteomics* 2005, *4*, 144–155.

[30] Echan, L. A., Tang, H. Y., Ali-Khan, N., Lee, K., Speicher, D. W., *Proteomics* 2005, *5*, 3292–3303.

[31] Roche, S., Tiers, L., Provansal, M., Seveno, M., Piva, M. T., Jouin, P., Lehmann, S., *J. Proteomics* 2009, *72*, 945–951.

[32] Bellei, E., Bergamini, S., Monari, E., Fantoni, L. I., Cuoghi, A., Ozben, T., Tomasi, A., *Amino Acids* 2010, *40*, 145–156.

[33] Cho, S. Y., Lee, E. Y., Lee, J. S., Kim, H. Y., Park, J. M., Kwon, M. S., Park, Y. K., Lee, H. J., Kang, M. J., Kim, J. Y., Yoo, J. S., Park, S. J., Cho, J. W., Kim, H. S., Paik, Y. K., *Proteomics* 2005, *5*, 3386–3396.

[34] Freeman, W. M., Lull, M. E., Guilford, M. T., Vrana, K. E., *Proteomics* 2006, *6*, 3109–3113.

[35] Govorukhina, N. I., Reijmers, T. H., Nyangoma, S. O., van der Zee, A. G., Jansen, R. C., Bischoff, R., *J. Chromatogr. A* 2006, *1120*, 142–150.

[36] Pieper, R., Su, Q., Gatlin, C. L., Huang, S. T., Anderson, N. L., Steiner, S., *Proteomics* 2003, *3*, 422–432.

[37] Vasudev, N. S., Ferguson, R. E., Cairns, D. A., Stanley, A. J., Selby, P. J., Banks, R. E., *Proteomics* 2008, *8*, 5074–5085.

[38] Maiese, K., Li, F., Chong, Z. Z., *J. Am. Med. Assoc.* 2005, *293*, 90–95.

[39] Eagleton, H. J., Littlewood, T. J., *Curr. Hematol. Rep.* 2003, *2*, 109–115.

[40] Faulds, D., Sorkin, E. M., *Drugs* 1989, *38*, 863–899.

[41] Barroso, O., Mazzoni, I., Rabin, O., *Asian J. Androl.* 2008, *10*, 391–402.

[42] Robach, P., Recalcati, S., Girelli, D., Gelfi, C., Aachmann-Andersen, N. J., Thomsen, J. J., Norgaard, A. M. et al., *Blood* 2009, *113*, 6707–6715.

[43] Lundby, C., Achman-Andersen, N. J., Thomsen, J. J., Norgaard, A. M., Robach, P., *J. Appl. Physiol.* 2008, *105*, 417–419.

[44] Karp, N. A., Kreil, D. P., Lilley, K. S., *Proteomics* 2004, *4*, 1421–1432.

[45] Karp, N. A., Lilley, K. S., *Proteomics* 2005, *5*, 3105–3115.

[46] Moriggi, M., Cassano, P., Vasso, M., Capitanio, D., Fania, C., Musicco, C., Pesce, Gadaleta, M. N., Gelfi, C., *Proteomics* 2008, *8*, 3588–3604.

[47] Tonge, R., Shaw, J., Middleton, B., Rowlinson, R., Rayner, S., Young, J., Pognan, F., Hawkins, E., Currie, I., Davison, M., *Proteomics* 2001, *1*, 377–396.

[48] Ernoult, E., Bourreau, A., Gamelin, E., Guette, C., *J. Biomed. Biotechnol.* 2010, *2010*, 927917.

[49] Anderson, N. L., Polanski, M., Pieper, R., Gatlin, T., Tirumalai, R. S., Conrads, T. P., Veenstra, T. D., Adkins, J. N., Pounds, J. G., Fagan, R., Lobley, A., *Mol. Cell. Proteomics* 2004, *3*, 311–326.

[50] Lilley, K. S., Razzaq, A., Dupree, P., *Curr. Opin. Chem. Biol.* 2002, *6*, 46–50.

[51] Leung, S. M., Pitts, R. L., *Methods Mol. Biol.* 2008, *441*, 57–70.

